

## Formation of Si(111)-(1×1)Cl

John J. Boland and J. S. Villarrubia\*

*IBM Research Division, Thomas J. Watson Research Center, P.O. Box 218, Yorktown Heights, New York 10598*

(Received 16 August 1989)

Using scanning tunneling microscopy, we have studied the structural modifications induced by Cl upon reaction with Si(111)-(7×7). At low coverages, reacted and unreacted sites are distinguishable in both current-voltage curves and topographs. At saturation coverage, annealing produces extensive mass transport in which most of the adatom layer is stripped away and accumulated in pyramidal Si structures, permitting the complete underlying Si rest-atom layer to be imaged. Much of this layer initially exists as nearly-adatom-free Cl-stabilized 7×7 domains, but further annealing converts it slowly to the more favorable bulklike 1×1 structure. Structures intermediate between the 7×7 and 1×1 are observed.

The interaction of Cl with Si surfaces is of great scientific and technological interest. Cl forms well-ordered overlayers on Si(111) and has become a model system for studying chemisorption on semiconductor surfaces.<sup>1-4</sup> Cl adsorption plays a key role in many technologically important processes such as reactive ion etching and chemical vapor deposition.<sup>5</sup> X-ray photoemission spectroscopy (XPS) studies of Cl on Si(111)-(7×7) show peaks due to Si bonded to multiple Cl atoms before annealing, but only to one afterwards.<sup>4</sup> Low-energy electron diffraction (LEED) structural studies show a disordered 7×7 pattern with some sharpening of the fractional-order spots after the anneal.<sup>4,5</sup> However, to date the surface structure giving rise to these disordered LEED patterns has been unknown.

We have annealed Si(111)-(7×7) surfaces that have been saturated with Cl and studied the resulting surface structures with the scanning tunneling microscope (STM). Chlorine ties up surface dangling bonds (DB's), which permits the Si-adatom layer to be stripped away, revealing the underlying rest-atom layer. Under some annealing conditions, much of this layer retains the original 7×7 reconstruction. The remainder is converted to 1×1 or other structures. In a previous paper<sup>6</sup> we concentrated on the 7×7 regions, reporting the direct observation of the stacking fault as well as electronic and geometrical differences between faulted and unfaulted domains.

In the present work, we concentrate on the formation of the 1×1 regions. We describe a process of conversion that begins with the reaction of submonolayer amounts of Cl with the adatom terminated 7×7, followed at saturation coverage by the stripping of the adatoms, their accumulation in protrusions on the surface, the conversion of Cl-terminated 7×7 domains into Cl-terminated 1×1 domains through several intermediate structures, and ultimately the nearly complete conversion of the surface to 1×1 domains.

This work was performed using an STM similar to that described by Demuth *et al.*,<sup>7</sup> which was mounted in an ion-pumped ultrahigh vacuum (UHV) chamber with a

base pressure of  $\sim 1 \times 10^{-10}$  Torr. The sample was a phosphorous-doped (1  $\Omega$  cm) Si(111) wafer that was out-gassed for 5 h at 700°C prior to removal of the surface oxide. (All sample temperatures reported here were measured using an ir pyrometer.) After cooling for several hours the 7×7 surface was generated by heating the sample to 1050°C for 30 s. Tips were fabricated from 0.01 in. wide wire that was electrochemically etched in a 2N NaOH solution. Prior to use the tips were heated to 600°C in a vacuum for 10 min to remove the electrolytic oxide. The Cl source was a solid-state AgCl electrochemical cell.<sup>8</sup> Measurements included both standard STM topographs taken in the constant-current mode and current-voltage characteristics (*I-V* curves) performed using the sample-and-hold technique developed by Feenstra *et al.*<sup>9</sup> Images displayed here are uncorrected for thermal drift.

At present the generally accepted structure of the 7×7 surface is the dimer-adatom-stacking-fault (DAS) model of Takayanagi *et al.*<sup>10</sup> In this model the reconstruction occurs over two surface layers and consists of a lower rest-atom double layer (shown in Fig. 1) that is capped by an adatom layer (not shown). The rest-atom layer contains 1×1 triangular subunits that are alternately faulted or unfaulted with respect to the bulk layer beneath. These subunits are bounded by dimer-row domain walls that intersect to produce holes at the corners of the cell. The outer adatom layer consists of 6 Si atoms arranged in a 2×2 structure within each triangular subunit. The 7×7 surface contains 19 DB's per unit cell, 12 of which are due to adatoms, six from unsaturated rest atoms, and one from a corner hole.

We first characterized Cl adsorption at coverages below saturation. Figure 2 shows topographs of the same area taken at sample biases below [Fig. 2(a)] and above [Fig. 2(b)] 2 V. Below 2 V, the reacted sites are darker than the unreacted ones. They appear to be depressions, or perhaps even vacancies, in the 7×7 structure. However, they are not vacancies, as can be seen in Fig. 2(b). Here at the higher bias, the contrast has reversed and the reacted sites appear to be brighter than the unreacted

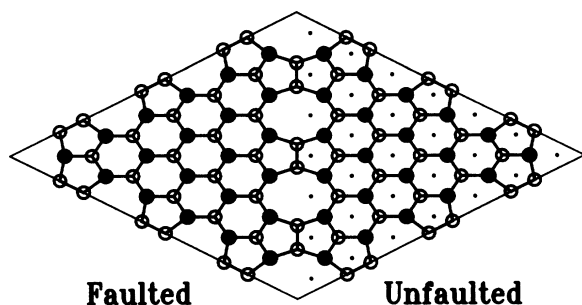


FIG. 1. Schematic of the DAS rest-atom double layer showing both the faulted and unfaulted subunits of the cell. The large solid and small open circles represent the upper and lower atoms in the double layer, respectively. Dots represent the atoms visible in the layer beneath the double layer. The adatom layer (not shown) consists of a local  $2 \times 2$  structure within each of the triangular subunits of the cell.

ones. This behavior is similar to that observed by Avouris and Wolkow<sup>11</sup> for the reaction of  $\text{NH}_3$  with  $\text{Si}(111)-(7 \times 7)$ .

The reason reacted sites appear to be depressions at

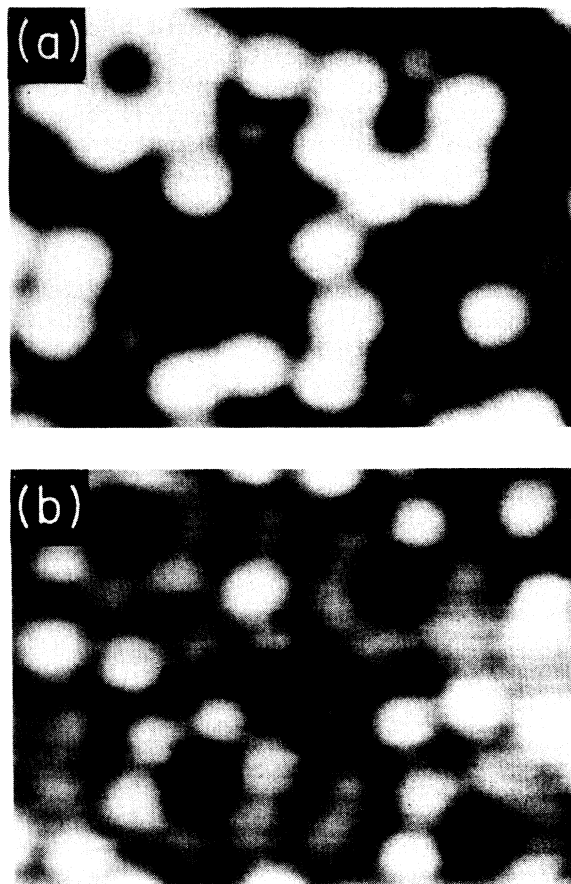


FIG. 2. Topographs of the same area of a reacted surface taken at sample biases of (a) +1 V and (b) +3 V. Note that adatoms that are dark in (a) are bright in (b) vice versa. The area shown is  $54 \times 40 \text{ \AA}^2$ .

low-sample bias can be seen in Fig. 3, which shows  $dI/dV$  curves that were taken in conjunction with topographs. Figure 3(a), taken over an unreacted corner adatom site (i.e., one next to a corner hole) has peaks just above and below the Fermi level arising from the adatom dangling-bond states, in agreement with earlier STM results.<sup>12,13</sup> Over a reacted corner adatom site [Fig. 3(b)] the corresponding peaks are almost completely absent. Similar results are obtained for the center adatoms. In Fig. 2(a), all of the tunneling current is contributed by electrons with energies between 0 eV (the Fermi level) and 1 eV (the maximum energy obtainable from the field). As Fig. 3 shows, the interaction of Cl with the Si-dangling bonds markedly reduces the density of states within this energy window. The result is that the tip must approach closer to the surface, in order to obtain the required tunneling current, creating the appearance of a vacancy.

The origin of the opposite contrast at the higher bias of Fig. 3(b) is not as readily apparent. Whatever is producing the extra tunneling current over the reacted sites is not a sharp feature that manifests itself as a peak in  $dI/dV$  curves as is indicated by the fact that the contrast in the topographs continually increased all the way out to 4 V, which is the highest bias for which we have data. We suggest that the additional current over these sites is due to tunneling into the tail of the Cl-derived  $\sigma^*$  state, formed by the bonding interaction between the Si-adatom dangling bond and the Cl  $3p$  orbital. On the Cl-terminated  $\text{Si}(111)-(1 \times 1)$  surface, this  $\sigma^*$  state is calculated to disperse in a band from about 2.5 to about 6 eV above the Fermi level.<sup>3</sup> This is a region of the surface Brillouin zone, where a projection of Si-bulk density of states is nonzero, so that further broadening of the  $\sigma^*$  state is expected due to hybridization with the bulk.

A survey of the reacted surface showed that there were approximately equal numbers of reacted corner and center adatom sites. Furthermore, under conditions in which most of the adatom sites had reacted,  $dI/dV$

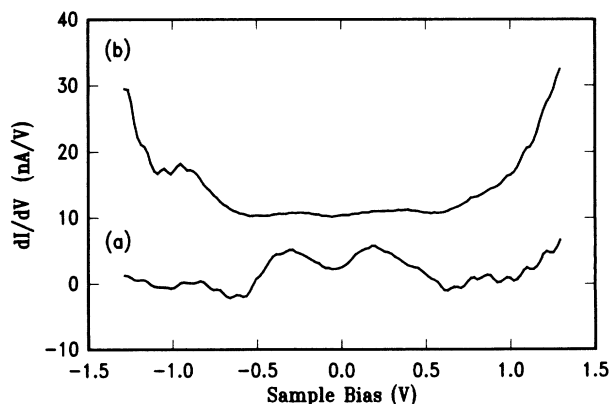


FIG. 3.  $I$ - $V$  characteristics measured over (a) unreacted and (b) reacted corner adatom sites. The feedback loop was stabilized at a tunneling current of 2 nA and a sample bias of +1 V. For clarity, the data in (b) has been displaced relative to that in (a).

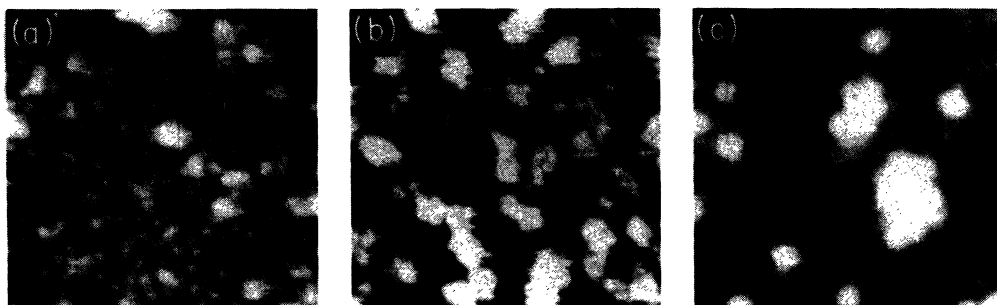


FIG. 4. Topographs of a Cl-saturated surface recorded at +3 V following an anneal at (a) 220°C for 5 s, (b) 300°C for 25 s, and (c) 470°C for 2 min. In (a) and (b) the area is  $127 \times 127 \text{ \AA}^2$ , while in the closeup (c) it is  $67 \times 67 \text{ \AA}^2$ .

curves failed to show the presence of any reacted rest-atom sites. These results are different from the relative site reactivities observed for the reaction of  $\text{NH}_3$  with this surface. The origin of this discrepancy may be due to the nature of our source, from which an appreciable fraction of the Cl occurs in the form of Cl atoms.<sup>14</sup> Such Cl atoms have a very small barrier to reaction and might react initially with the outermost surface-adatom layer.

Figure 4 is a series of topographs at saturation Cl coverage and progressively higher annealing temperatures. Figure 4(a) was taken after a Cl exposure 100 times greater than that used to produce the coverage in Fig. 2, followed by a mild anneal to approximately 220°C for 5 s. Apart from a few protrusions, the surface resembles the clean Si(111)-(7×7) surface, and one might be tempted to conclude that it remains largely unreacted. However, the resemblance is misleading. *I-V* characteristics taken over the adatoms in this structure lack the dangling-bond peaks near 0.5 and -0.5 eV. That is, the *I-V* curves are like Fig. 3(b), not Fig. 3(a). The surface is saturated with Cl.

Without further Cl exposure, annealing to 300°C for 25 s increases the size and number of protrusions and removes the adatoms from the regions between them, as shown in Fig. 4(b). The 7×7 periodicity, with the diamond-shaped unit cell composed of crisscrossed dimer rows terminating in corner holes, is preserved. However, as we showed in our previous work,<sup>6</sup> instead of the 12 maxima per unit cell characteristic of the unreacted 7×7, these unit cells contain 42 maxima, as is characteristic of the rest-atom layer (Fig. 1).

With anneals between 370 and 390°C, we begin to observe the “unreconstruction” of the surface, as portions of it revert to a bulklike 1×1 pattern. This appears to be a kinetically rather slow process, so that even with annealing temperatures of 470°C for 2 min, as in Fig. 4(c), there is a substantial coexistence of 7×7 with 1×1 and other structures.

In Fig. 4(c), which is a closeup of the annealed surface, the triangular region at the bottom of the image is an isolated faulted piece of a 7×7 unit cell from which five of the six adatoms have been removed. It is clear from the unobstructed part that the triangle is equilateral with six atoms on each side. The maxima corresponds to the positions of the outermost atoms of the DAS rest-atom dou-

ble layer (Fig. 1). The protrusion at the lower left corner is the one remaining adatom. It is situated in the three-fold hollow in that corner, the same position it occupies on the unreacted 7×7 surface. Note that this triangular region is bounded by the same dimer rows and corner holes that delineate segments of unit cells in the 7×7 structure. As was the case for the adatoms prior to the anneal, *I-V* curves taken over the rest-atom layer on these Cl-saturated surfaces invariably indicate that the bonds out of the surface are tied up by Cl.

Within the rest-atom layer, the 7×7 structure is essentially a 1×1 pattern broken at regular intervals by dimer rows that intersect at corner holes. Adjacent to the triangular region in Fig. 4(c) is an extended 1×1 region, unbroken by dimer rows. This region extends for over 100 Å (not all of which is shown) away from the faulted triangle. In the larger image of which Fig. 4(c) is a subset, such 1×1 domains occupied approximately 30% of the surface, with most of the rest consisting of 7×7 domains and protrusions.

A three-dimensional rendering of one of the protrusions is shown in Fig. 5. The top layer of this object is 6.5 Å above the rest-atom layer and contains ten atoms in a triangle with four atoms per side. These ten atoms are above another layer of atoms, which in turn sits on the rest-atom layer. The middle layer of atoms is larger than the topmost one, forming a ledge that runs around the perimeter of the object. On the right side of Fig. 5 this ledge is about the expected height (3.13 Å) for a step on the Si(111) surface. On the left, where the ledge bridges a dimer row in the rest-atom layer, the ledge is double, with plateaus at 5.0 Å and 2.2 Å. By constructing a model of this object, we estimate that it contains 60 atoms. This number is consistent with its volume and the bulk density of Si.

The appearance of the protrusions simultaneously with the disappearance of adatoms from other parts of the surface suggests that the protrusions represent accumulations of former adatoms. Because of their high density, the protrusions together with the remaining individual adatoms account for about 65% of the adatoms originally on the surface on typical areas we have examined. Some of the remaining adatoms can be accounted for by the reversion of parts of the surface to unreconstructed domains, since it requires eight atoms per 7×7 unit cell

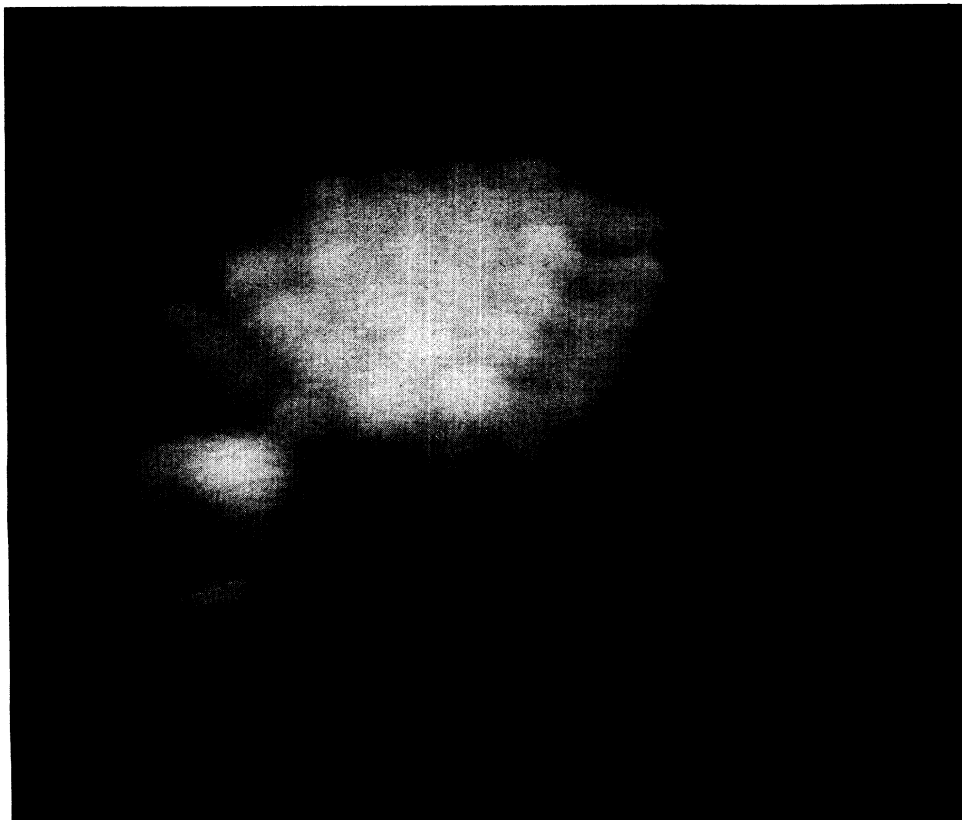


FIG. 5. Three-dimensional rendering of a surface protrusion. The image is  $39 \times 39 \text{ \AA}^2$  in size and was recorded at +2 V with a tunneling current of 0.35 nA.

to remove the dimer rows. The protrusions, the conversion of  $7 \times 7$  to  $1 \times 1$  domains, and the remaining individual adatoms together account for over 90% of the adatoms originally in the region of which Fig. 4(c) is a part. Thus, while small amounts of Si removal by Cl cannot be ruled out, the vast majority of the adatoms remain on the surface at these temperatures.

The variety of surface structures in Fig. 4(c), all coexisting within less than  $100 \text{ \AA}$  of each other, is striking. Without Cl on the surface, adatom terminated and under-terminated rest-layer structures would have markedly different energies. This is because the adatoms serve to satisfy Si-dangling bonds that otherwise make a

significant contribution to the surface energy.<sup>15</sup> With Cl saturating the surface, there are no unsatisfied bonds in any of these structures, and the energy differences between them are reduced.

The formation of dimer-row domain walls and capping the rest layer with Si adatoms reduces the number of dangling bonds from 49 to 19. Despite the fact that this reconstruction requires the formation of corner holes and a stacking fault which are, considered in isolation, energetically unfavorable, the dangling-bond reduction provides a sufficient reduction in energy to make the net energy change favor reconstruction.<sup>15</sup> With passivation of dangling bonds by Cl, the dangling-bond contribution to

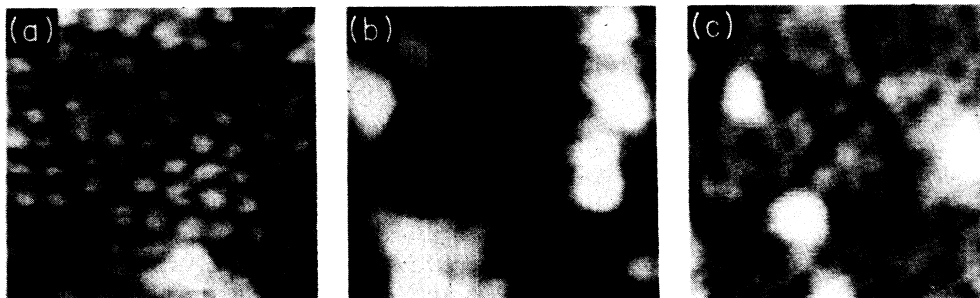


FIG. 6. Topographs showing faulted triangular subunits with (a) five, (b) four, and (c) three atoms per side. In each case the images were recorded at a bias of +2 V and the areas shown are  $35 \times 35 \text{ \AA}^2$ .

the surface energy is removed with the result that removal of adatoms, corner holes, and stacking faults, leading to a bulklike  $1 \times 1$  termination, becomes favored.

Intuitively, removal of the adatoms into the protrusions on the surface is the kinetically easier part of this process, so it is not surprising that it proceeds at the lower temperature. The adatom layer is relatively open, with adatoms  $7.68 \text{ \AA}$  apart, allowing plenty of room for Cl (atomic radius  $0.97 \text{ \AA}$ ) to penetrate and insert itself into the bonds between the adatoms and the rest-atom layer. Furthermore, the adatoms can diffuse individually into the protrusions.

By contrast, removal of the dimer-row domain walls and concomitant stacking faults in the rest layer requires configurational changes involving many atoms. The smallest step between two stable configurations that we can imagine would involve a reduction in the size of one of the faulted triangles by all or part of one row. Reduction by part of a row would leave a kinked boundary between faulted and unfaulted domains. Such kinks are generally energetically costly, and we have not observed them. We have, however, observed triangular-faulted domains with fewer than the  $7 \times 7$  domains canonical six rows of atoms, some of which are shown in Fig. 6. These

triangular structures do not occur with the same relative frequency on the surface; triangles with five and three atoms per side are common, while those with four atoms per side are seldom observed. Presumably, this is related to the fact that triangles with an even number of atoms per side require a disruption of the eight membered rings that make up the domain walls (see Fig. 1). For the sake of completeness, and despite the poor quality of the data, we include in Fig. 6 a topograph that shows a triangle with four atoms per side. In each case the faulted triangular structure arises from the progressive stepwise motion of the dimer-row domain walls. For example, after a single step the faulted subunit consists of an equilateral triangle with five atoms per side, while after two steps it has four atoms per side and so on. As the dimer row advances and the size of the unfaulted region grows, the length of the domain wall surrounding the faulted subunit diminishes. This process continues until the dimer-row domain wall is annihilated when it reaches the corner hole of the cell.

Annealing at still higher temperatures begins to cause the loss of Cl from the surface via thermal desorption of  $\text{SiCl}_2$  and  $\text{SiCl}_4$  fragments.<sup>16</sup> This is accompanied by the dispersal of the adatoms from the protrusions back to the

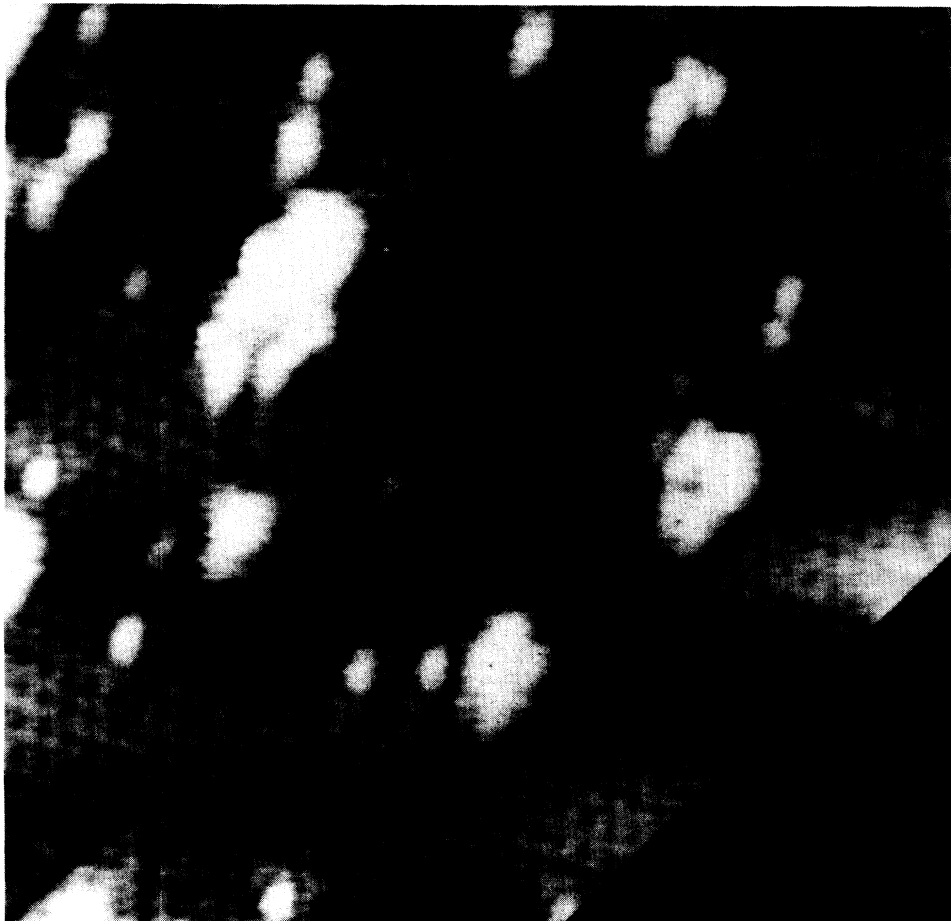


FIG. 7. Topograph of the surface obtained after exposure to Cl while the sample was held at  $550^\circ\text{C}$ . The image was recorded at a bias of  $+2 \text{ V}$  and the area shown is  $110 \times 110 \text{ \AA}^2$ . Note there is substantial thermal drift in this image.

rest of the surface. By flashing the crystal to 1050 °C for a few seconds, we have been able to return the surface to the  $7\times 7$  pattern with  $I-V$  curves normal for unreacted Si. Because the Cl-terminated surface is highly unreactive, passivation with Cl followed after some period of time by restoration of the  $7\times 7$  domains via thermal desorption has proved to be a useful method of preserving a clean  $7\times 7$  surface in vacuum for periods of several weeks.

We have seen that annealing the sample increases the fraction of the surface with this bulk-terminated structure indicating that it is the thermodynamically stable form of the Si(111)-( $7\times 7$ ) Cl surface. The presence of the  $7\times 7$  domains in Fig. 4 are due to the slow rate of conversion to the  $1\times 1$  structure. It is possible to achieve quantitative conversion of the surface to the  $1\times 1$  structure by prolonged annealing or by dosing with Cl while the Si crystal is held at the anneal temperature. This is clearly demonstrated in Fig. 7, which shows a large area Cl-stabilized  $1\times 1$  region with some remnants of the  $7\times 7$  structure.

In this work we have presented an STM study of the scientifically and technologically important interaction of Cl with Si. At low coverages we have shown that reacted

Si atoms are distinguishable from unreacted ones in topographs and by their  $I-V$  characteristics and that the interaction involves the adatom dangling-bond states. At higher coverages the Cl penetrates the adatom structure and inserts itself in the bonds between the adatom and rest-atom layers. As a result there is extensive mass transport on the surface in which the Cl serves to stabilize various surface structures. In particular, after saturation coverage followed by an anneal, the adatoms are stripped from large areas of the surface and accumulated in structures that are generally triangular in cross section and two double-layers high. In the areas vacated by the adatoms, we have obtained complete images of the underlying rest-atom layer. Initially much of this layer existed in the form of Cl-passivated adatomless  $7\times 7$  domains. However, after prolonged annealing this surface slowly reverted to the more favorable Cl-stabilized bulk-terminated structure. The transition between these structures is sufficiently slow that isolated intermediate structures are observed corresponding to the stepwise progressive motion of the dimer-row domain walls. Under appropriate annealing conditions it is possible to quantitatively convert the surface to the bulk-terminated structure.

---

\*Present address: National Institute of Standards and Technology, Gaithersburg, Maryland 20899.

<sup>1</sup>J. E. Rowe, G. Margaritondo, and S. B. Christman, *Phys. Rev. B* **16**, 1581 (1977).

<sup>2</sup>P. H. Citrin, J. E. Rowe, and P. Eisenberger, *Phys. Rev. B* **28**, 2299 (1983).

<sup>3</sup>M. Schlüter and M. L. Cohen, *Phys. Rev. B* **17**, 716 (1978).

<sup>4</sup>R. D. Schnell, D. Rieger, A. Bogen, F. J. Himpsel, K. Wandelt, and W. Steinmann, *Phys. Rev. B* **32**, 8057 (1985).

<sup>5</sup>W. Sesselmann and T. J. Chuang, *J. Vac. Sci. Technol. B* **3**, 1507 (1985).

<sup>6</sup>J. S. Villarrubia and J. J. Boland, *Phys. Rev. Lett.* **63**, 306 (1989).

<sup>7</sup>J. E. Demuth, R. J. Hamers, R. M. Tromp, and M. E. Welland,

*J. Vac. Sci. Technol. A* **4**, 1320 (1986).

<sup>8</sup>R. D. Schnell, D. Rieger, A. Bogen, K. Wandelt, and W. Steinmann, *Solid State Commun.* **53**, 205 (1985).

<sup>9</sup>R. M. Feenstra, J. A. Stroscio, and A. P. Fein, *Surf. Sci.* **181**, 295 (1986).

<sup>10</sup>K. Takayanagi, Y. Tanishiro, S. Takahashi, and M. Takahashi, *Surf. Sci.* **164**, 367 (1985).

<sup>11</sup>Ph. Avouris and R. Wolkow, *Phys. Rev. B* **39**, 5091 (1989).

<sup>12</sup>R. J. Hamers, R. M. Tromp, and J. E. Demuth, *Phys. Rev. Lett.* **56**, 1972 (1986).

<sup>13</sup>R. Wolkow and Ph. Avouris, *Phys. Rev. Lett.* **60**, 1049 (1988).

<sup>14</sup>H. M. Kramer and E. Bauer, *Surf. Sci.* **107**, 1 (1981).

<sup>15</sup>D. Vanderbilt, *Phys. Rev. B* **36**, 6209 (1987).

<sup>16</sup>S. M. George (private communication).

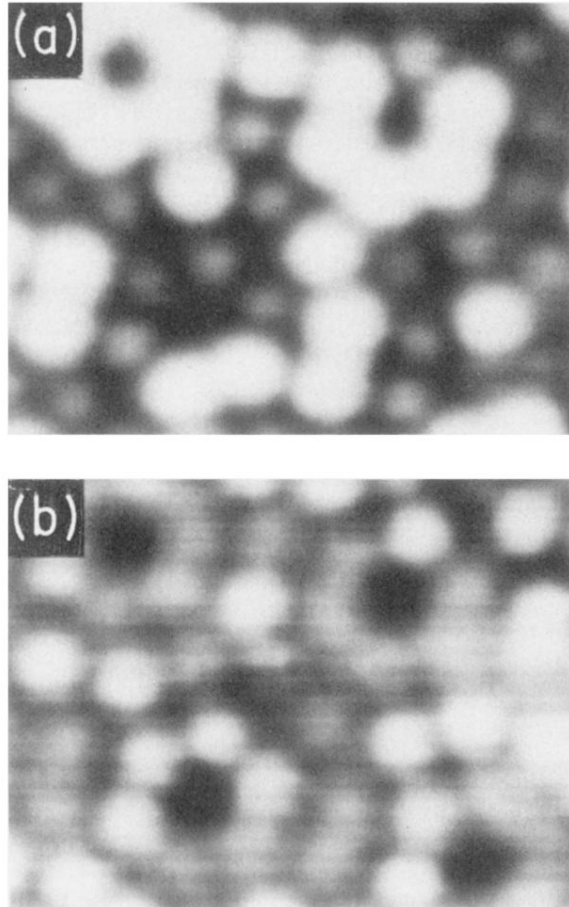


FIG. 2. Topographs of the same area of a reacted surface taken at sample biases of (a) +1 V and (b) +3 V. Note that adatoms that are dark in (a) are bright in (b) vice versa. The area shown is  $54 \times 40 \text{ \AA}^2$ .

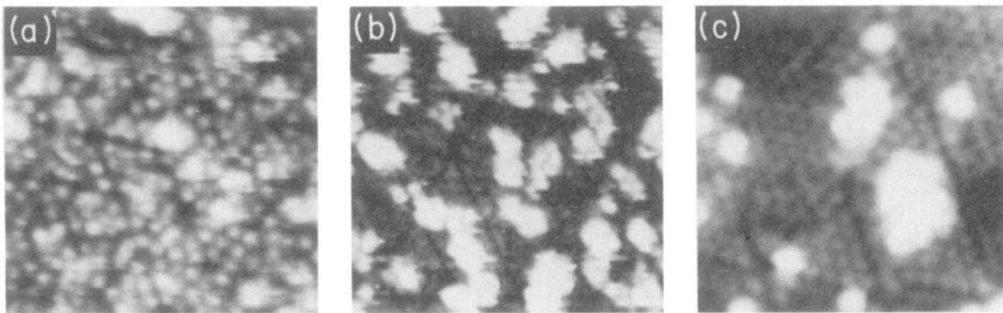


FIG. 4. Topographs of a Cl-saturated surface recorded at +3 V following an anneal at (a) 220 °C for 5 s, (b) 300 °C for 25 s, and (c) 470 °C for 2 min. In (a) and (b) the area is  $127 \times 127 \text{ \AA}^2$ , while in the closeup (c) it is  $67 \times 67 \text{ \AA}^2$ .



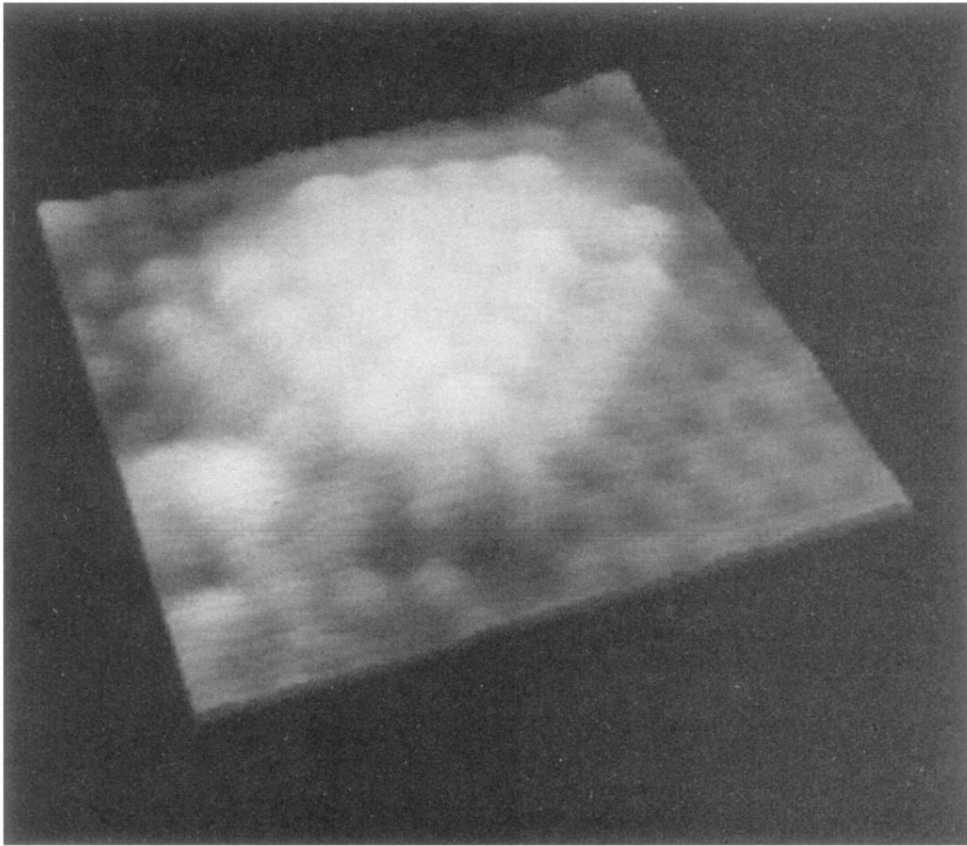


FIG. 5. Three-dimensional rendering of a surface protrusion. The image is  $39 \times 39 \text{ \AA}^2$  in size and was recorded at +2 V with a tunneling current of 0.35 nA.

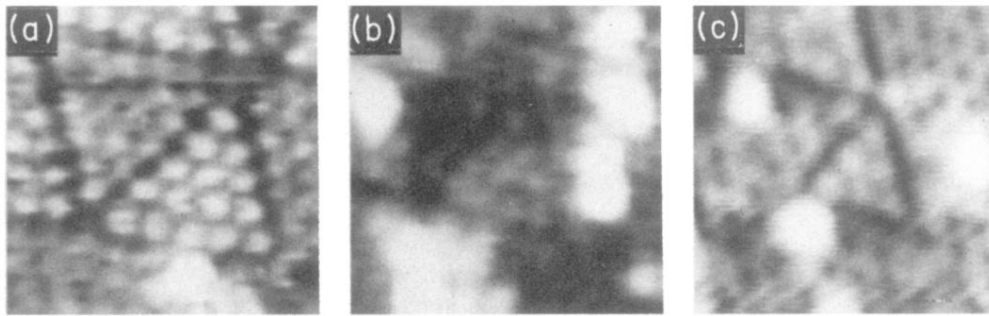


FIG. 6. Topographs showing faulted triangular subunits with (a) five, (b) four, and (c) three atoms per side. In each case the images were recorded at a bias of +2 V and the areas shown are  $35 \times 35 \text{ \AA}^2$ .

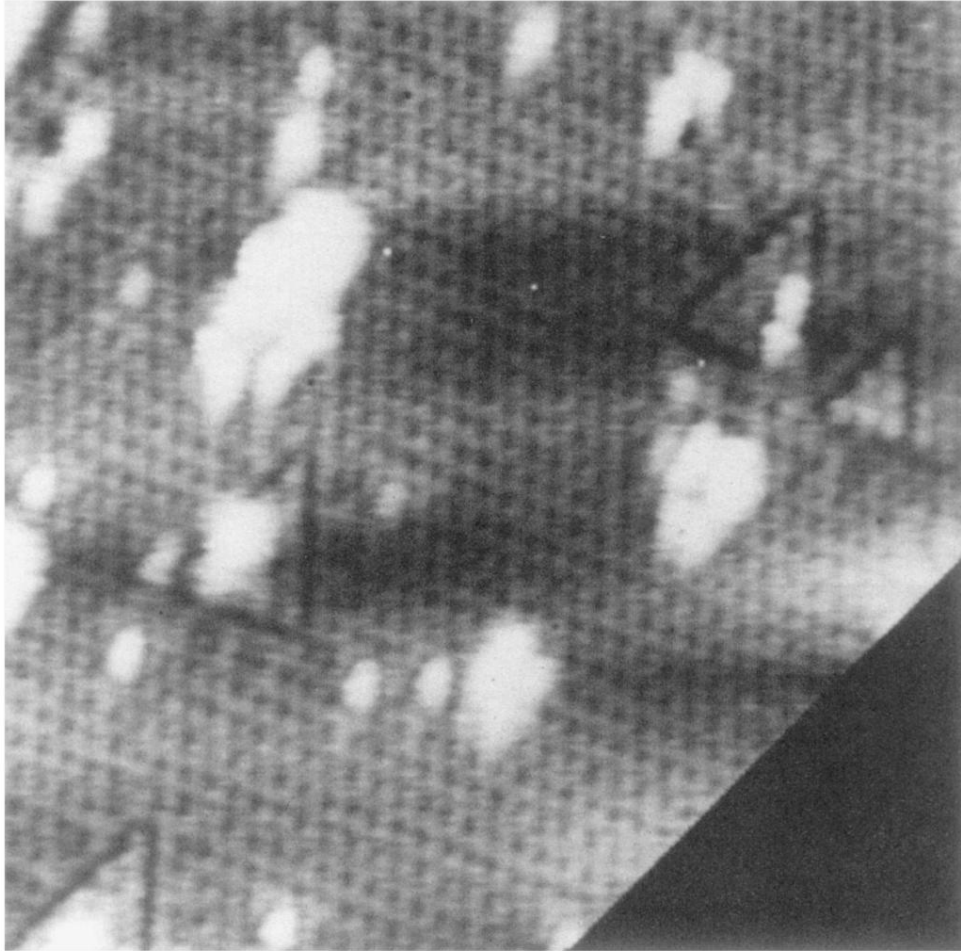


FIG. 7. Topograph of the surface obtained after exposure to Cl while the sample was held at 550 °C. The image was recorded at a bias of +2 V and the area shown is  $110 \times 110 \text{ \AA}^2$ . Note there is substantial thermal drift in this image.